Journal of Earth Science, *Vol. 28*, *No. 3*, *p. 433–446*, *June 2017* *ISSN 1674-487X*
Printed in China
DOI: 10.1007/s12583-016-0934-1

Age, Genesis, and Tectonic Setting of the Mo-W Mineralized Dongshanwan Granite Porphyry from the Xilamulun Metallogenic Belt, NE China

Xuebing Zhang[1], **Keyong Wang**[*1], **Chengyang Wang**[2], **Wen Li**[3], **Qi Yu**[4], **Yicun Wang**[1], **Jianfeng Li**[5], **Duo Wan**[1], **Guanghuan Huang**[3]

1. *College of Earth Sciences*, *Jilin University*, *Changchun* 130061, *China*
2. *Department of Earthquake Science*, *Institute of Disaster Prevention Science and Technology*, *Beijing* 101601, *China*
3. *Inner Mongolia Shandong Gold Minerals Survey Co. Ltd.*, *Chifeng* 024005, *China*
4. *Heilongjiang Institute of Regional Geology Survey*, *Harbin* 150080, *China*
5. *College of Urban and Environmental Sciences*, *Liaoning Normal University*, *Dalian* 116029, *China*

Xuebing Zhang: http://orcid.org/0000-0001-7332-4338; Keyong Wang: http://orcid.org/0000-0002-7764-2074

ABSTRACT: The Xilamulun molybdenum polymetallic metallogenic belt in eastern Inner Mongolia forms one of the most important Mo metallogenic belts in northeastern China. The Dongshanwan porphyry Mo-W polymetallic deposit, in the northeastern part of the Xilamulun metallogenic belt, occurs along the periphery of a granite porphyry and consists of Mo-W-Ag sulfide and oxide disseminations and veinlets in hydrothermal assemblages. LA-ICP-MS zircon U-Pb dating of the Dongshanwan granite porphyry yields a crystallization age of 142.15±0.91 Ma, whereas molybdenite Re-Os isotopic dating model ages are of 139.9–141.5 Ma and an isochron age is of 140.5±3.2 Ma (MSWD=1.2). The age consistency indicates that the Dongshanwan deposit was a product of Early Cretaceous magmatism. The Dongshanwan granite porphyry is a high-alkali high-potassium intrusion and has high SiO_2 (75.39 wt.%–76.15 wt.%), low Al_2O_3 (12 wt.%–13 wt.%), Ba, Ti, P, and Sr contents, with negative Eu anomalies. The Y/Nb ratios are comparable to those of average continental crust and island arc basalts, corresponding to type-A2 granites. Our geochemical data indicate that the granite porphyry emplaced in an Early Cretaceous post-orogenic extensional environment following Mongol-Okhotsk oceanic subduction and subsequent continental collision.

KEY WORDS: Dongshanwan porphyry Mo-W deposit, zircon U-Pb dating, Re-Os dating, geochemistry, Xilamulun metallogenic belt.

0 INTRODUCTION

The Xilamulun metallogenic belt of Inner Mongolia extends 400 km for E-W strike in a transition zone between the North China and Siberian cratons (Fig. 1). The belt is superimposed by the Mongol-Okhotsk orogenic belt and the circum-Pacific tectonic regime in the Mesozoic (Xu et al., 2013; Wu et al., 2000). Four types of polymetallic Mo mineralization are recognized in the belt: porphyry, quartz vein, volcanic-hosted, and greisen (Zeng et al., 2011). Zircon U-Pb dating and Re-Os isotopic results indicate that the mineralization occurred in the different periods (Zhang J H et al., 2010; Zhang Z L et al., 2009; Chen et al., 2008; Wu H Y et al., 2008; Nie et al., 2007). In recent years, more than 10 medium-large-sized Mo-Cu polymetallic deposits have been discovered in the metallogenic belt which contains the Aolunhua, Banlasan, Xiaodongou, Nianzigou deposits. The Xilamulun metallogenic belt is favorable to explore new ore deposits.

The recently discovered Dongshanwan deposit, situated in the northern part of the Xilamulun metallogenic belt, is the representative of the porphyry-type Mo-W polymetallic deposits in the Xilamulun metallogenic belt. Zhao and Zhang (1994) reported the Rb-Sr whole-rock age for the granite porphyry of 134 Ma and considered that the Dongshanwan deposit was of the greisen type deposit, originating in the Early Cretaceous. Fu and Chen (2004) reported that the Dongshanwan ore bodies have existed regularity on planar and inclined aspects, and the ore veins in vertical direction were various types, including linear veins, thin veins, and wide veins. Xu et al. (2012) reported that the metallogenic mineralization was controlled by strata, plutons and fractures. Zeng et al. (2015) reported the Late Jurassic ore-forming ages of the deposit, and discussed the tectonic setting of the ore-forming. Whereas, the chronology of formation of the Dongshanwan deposit is necessary to be further defined. So, we use ICP-MS zircon U-Pb analyses and Re-Os isotopic analyses to determine

*Corresponding author: wangky@jlu.edu.cn

Manuscript received May 17, 2015.
Manuscript accepted April 27, 2016.

Zhang, X. B., Wang, K. Y., Wang, C. Y., et al., 2017. Age, Genesis, and Tectonic Setting of the Mo-W Mineralized Dongshanwan Granite Porphyry from the Xilamulun Metallogenic Belt, NE China. *Journal of Earth Science*, 28(3): 433–446. doi:10.1007/s12583-016-0934-1. http://en.earth-science.net

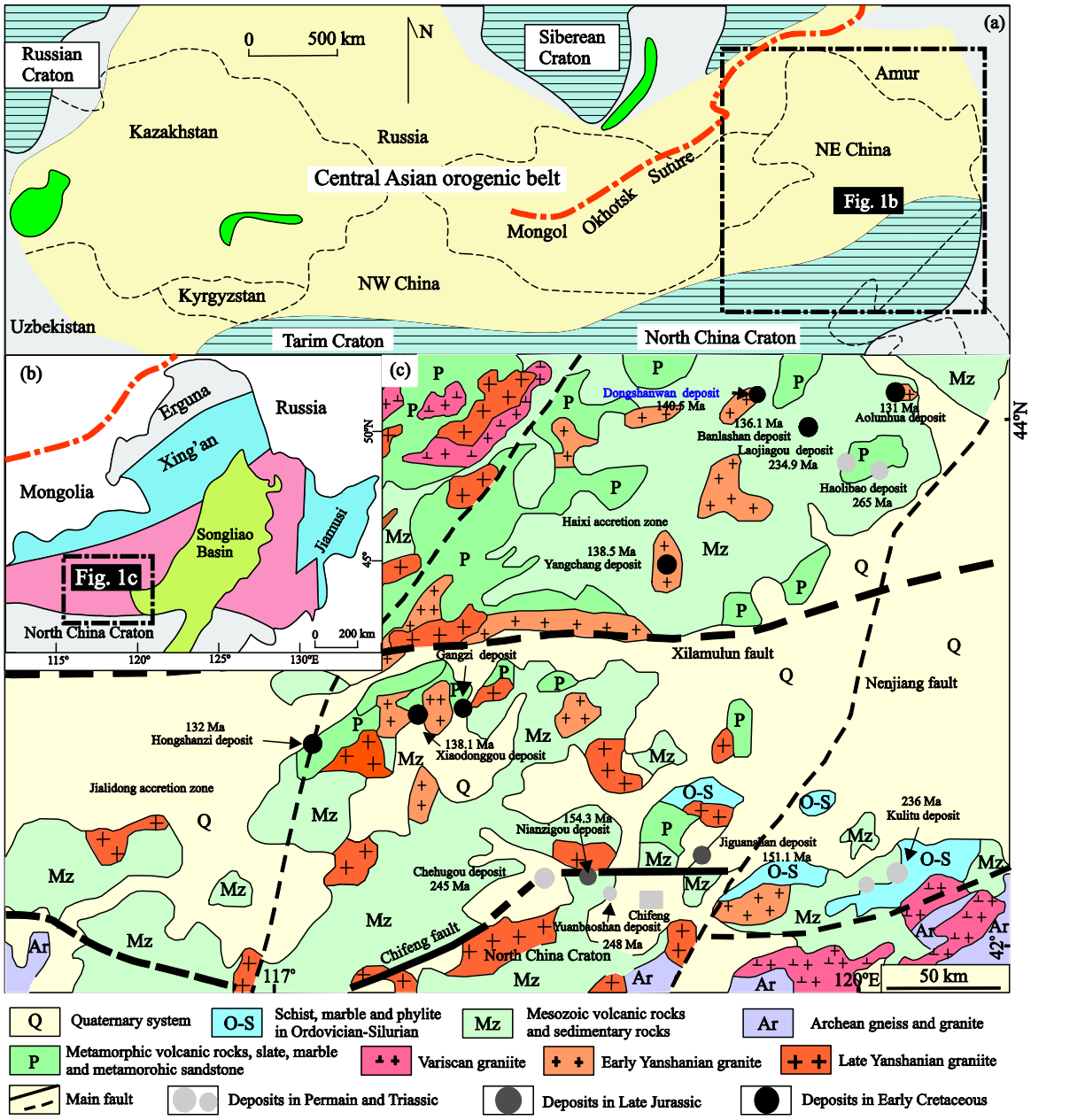

Figure 1. (a) Schematic map of the Central Asian orogenic belt (modified after Shen et al., 2010); (b) simplified geotectonic division of northeastern China (after Zhang J H et al., 2010); (c) geological map of the Xilamulun Mo belt (modified after Zeng et al., 2009).

the age of the granite porphyry and the age of the mineralization, respectively. What's more, the tectonic setting and mineralization mechanism of Xilamulun metallogenic belt is discussed.

1 GEOLOGICAL SETTING

1.1 Regional Geology

Tectonically, the Xilamulun metallogenic belt is located in the southern segment of the Great Xing'an Range (Fig. 1; Zhang et al., 2016). During the Paleozoic, the region experienced the evolution and final closure of the Paleo-Asian Ocean (Ding et al., 2016; Windley et al., 2007; Jahn et al., 2000). During the Mesozoic, the region experienced overprinting of the Mongol-Okhotsk tectonic regime in the northwest and circum-Pacific tectonic regime in the east (Li et al., 2004; Zhao et al., 1994). Therefore, the Mo mineralization in the Xilamulun metallogenic belt mainly formed in the Late Permain to Triassic (265–235 Ma), Late Jurassic (154–151 Ma), and Early Cretaceous (145–130 Ma) (Duan et al., 2015; Zeng et al., 2014, 2013, 2012, 2011, 2010a, b; Liu J M et al., 2010; Ma et al., 2009; Nie et al., 2007).

Strata outcropping in the Xilamulun metallogenic belt includes Permian strata, Upper Jurassic strata, and Quaternary. The Permian strata is mainly a sequence of basic-acidic volcanics and neritic-facies sedimentary rocks, comprising the Dashizhai, Zhesi, and Linxi formations. Lithologically, the Dashizhai Formation consists of sandstone, slate, lava, and tuff; the Zhesi Formation consists of sandstone, slate, felsic hornfels, and volcanic lava; the Linxi Formation consists of sandstone, mudstone-shale interbedded with slate, and tuff-bearing breccia.

The Jurassic strata include the Manketou'ebo, Xinmin, Manitu, and Baiyingao formations, which consist of lava flows, pyroclastics, and minor sandstone and shale lithologically (Zhang, 2009). Magmatic rocks include Variscan and Yanshanian intrusions, and Yanshanian granitoids associated with W, Mo, Pb, and Zn polymetallic mineralization in the Xilamulun metallogenic belt. Variscan intrusions include the Chehugou granite porphyry, the Harigentai moyite, and the Mengentaolegai plagiogranite. Yanshanian intrusions are widely distributed in the area and include the Aolunhua adamellite, the Dongshanwan granite porphyry, and the Budunhua granodiorite (Xin, 2013).

1.2 Ore Deposits

1.2.1 Ore deposit geology

The Dongshanwan deposit is situated in Balinzuoqi County of Inner Mongolia and located in the north of the Xilamulun fault. Strata outcropping in the Dongshanwan ore district includes the middle and under segments of the Lower Permian Zhesi Formation, the Lower Permian Dashizhai Formation, the lower segment of the Upper Jurassic Manketou'ebo Formation, and Quaternary (Fig. 2). The middle segment of the Permian Zhesi Formation, occurring in the southern part of ore blocks I and II, is composed of spotted slate, silty argillaceous slate, clay slate, metamorphosed fine sandstone, and siltstone lenses. This segment is 1 448 m thick, which dips 45°–75° to the northwest. The lower segment of the Lower Permian Zhesi

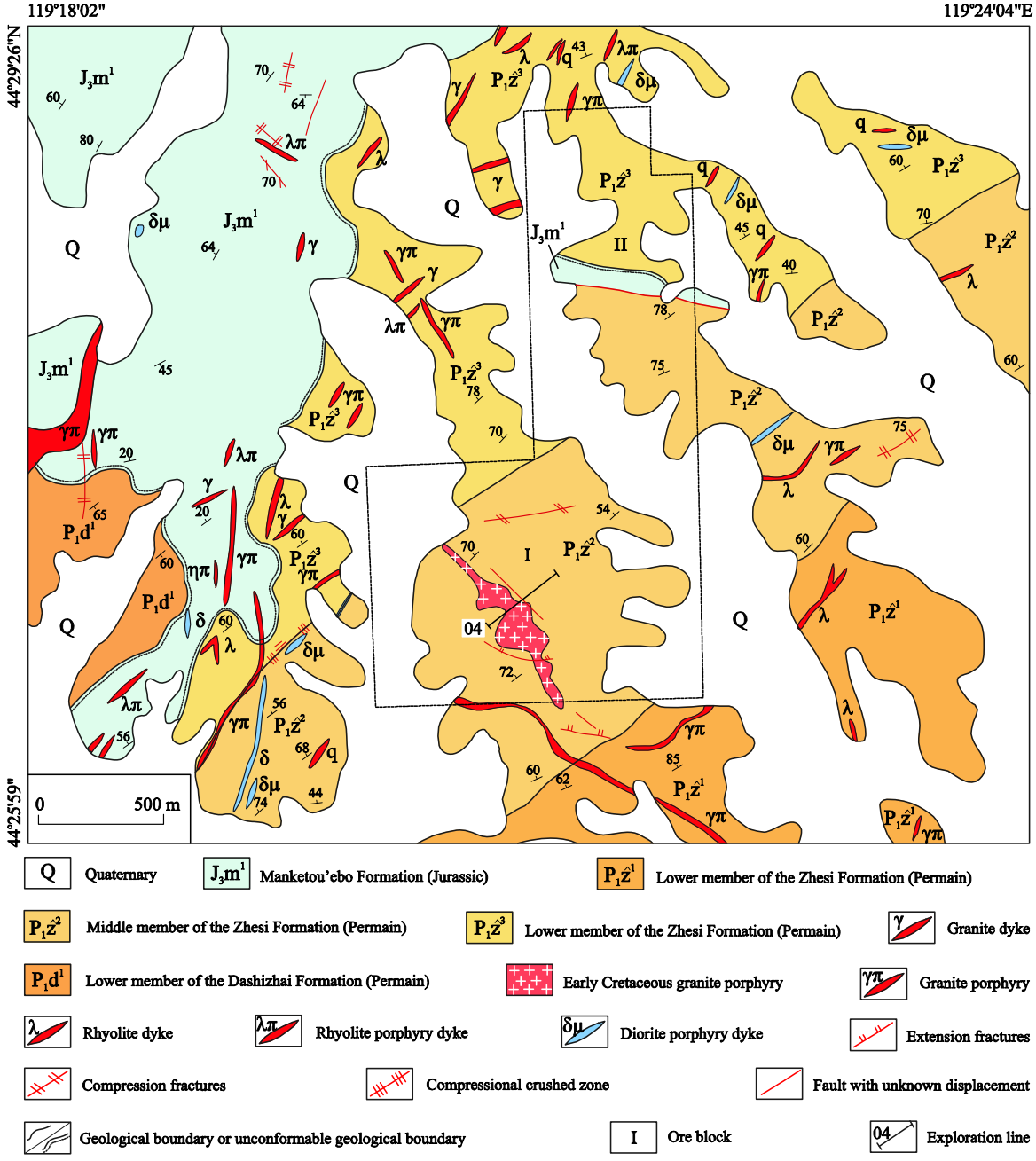

Figure 2. Geological map of the Dongshanwan Mo-W deposit.

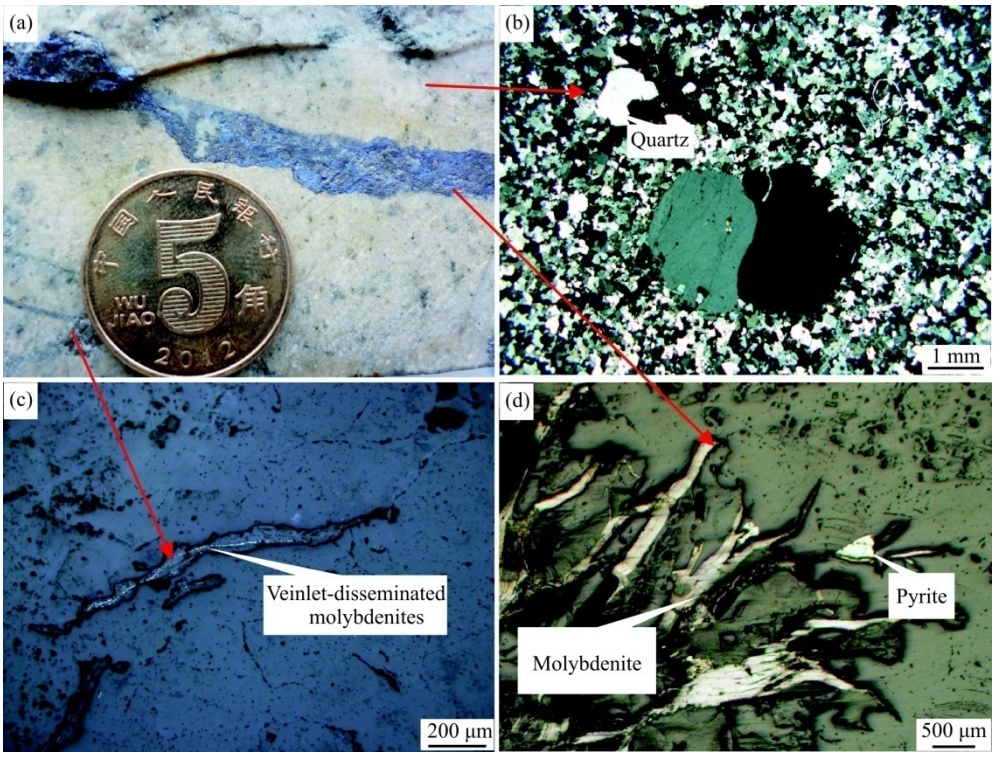

Figure 3. Molybdenum mineralization and photomicrograph of granite porphyry from the Dongshanwan deposit. (a) Pyrite-molybdenum-quartz vein; (b) photomicrograph of granite porphyry; (c) veinlet-disseminated molybdenite-quartz vein; (d) molybdenite and pyrite are symbiotic.

Formation, exposing in the northern part of ore block II, is composed of interbedded dark to light gray metamorphosed fine sandstone, siltstone, and argillite, this formation strikes to the northeast and dips 52º–75º to the northwest. The Lower Permian Dashizhai Formation, which occurs in the western part of the Dongshanwan deposit, consists of andesite, breccia-bearing tuff, and slate, this formaion strikes to the northeast and dips 60º–70º to the southeast. The lower segment of the Upper Jurassic Manketou'ebo Formation, which is exposed in the northern part of the Dongshanwan deposit and rests unconformably on the Lower Permian Zhesi Formation, is composed of rhyolitic volcanic breccia, rhyolitic tuff breccia, and rhyolitic vitric crystal tuff. The ore-hosting strata are the Lower Permian Zhesi Formation, which consists of spotty slate, silty shale, and slate.

Faults in the ore district are well developed, and can be grouped into NE-, NNW-, and EW-trending sets (Fig. 2). The NNW-trending faults are mainly located in ore block I, and dip to the southwest with the angles from 45º to 75º. The largest NNW-trending fault is 1 300 m long and 30–280 m wide, which is the main ore-controlling structure. The NE-trending faults are mainly located in ore block II, and dip to the northwest with the angles from 60º to 75º. The largest fault in this set, which is 100 m long and several tens of centimeters to several tens of meters wide, is an ore-controlling structure. The EW-trending faults are located in ore blocks I and II, and dip to the north with the angles from 60º to 80º, which cut the ore body.

The exposed intrusion in the ore district is solely granite porphyry, which is present as stock (Fig. 2). Granite porphyry contains about 10% phenocrysts, consisting of alkali feldspar (~60%), quartz (~20%), and hornblende (~10%); the rest is groundmass including alkali feldspar (~65%), plagioclase (~5%), quartz (~25%), and hornblende (~5%) (Fig. 3b). Fine-grained (felsophyric) granite buried in the granite porphyry. The dykes include diorite, granite porphyry, rhyolitic porphyry dykes, and quartz veins.

1.2.2 Mineralization characteristics

The layered or lenticular Mo mineralization mainly occurs in the endo- or exo-contact zones of granite porphyry (Fig. 3). The distribution of economic ore bodies indicate that the Dongshanwan deposit can be divided into two ore blocks. Ore block I is well developed and contains 152 economic ore bodies, which presently are sources of W, Mo, and Ag. This ore block is 1 052 m long, and the NW-trending orebodies dip to the southwest with the angles from 35º to 75º. Ore block II contains only one economic ore body, which presently consists of W, Mo, and Ag mineralization. The deposits of economic ores mainly contain Mo, W, Ag, Pb, and Zn ores (Li et al., 2010).

Mineralization and zonation are well developed in the Dongshanwan deposit. Alteration zones are developed at endo- or exo-contact zones of granite porphyry, including potassic zone, phyllitic zone, and propylitization zone (Fig. 4), and it is similar to typical porphyry alteration and zonation (Lowell and Guilbert, 1970). Alteration of the potassic zone includes potash feldspathization, sericitization, and silicification, and is mainly related to Mo and W mineralization. Alteration of the phyllitic zone includes silicification, kaolinization, and albitization, and is mainly related to multiple metal-bearing minerals, including wolframite, cassiterite, scheelite, argentite, galena, sphalerite, etc.. Propylitization zone alteration includes chloritization, carbonation, and silicification, and it only contains a few Ag multi-metal mineralizations. Compared with mineralization in the wall rocks, the

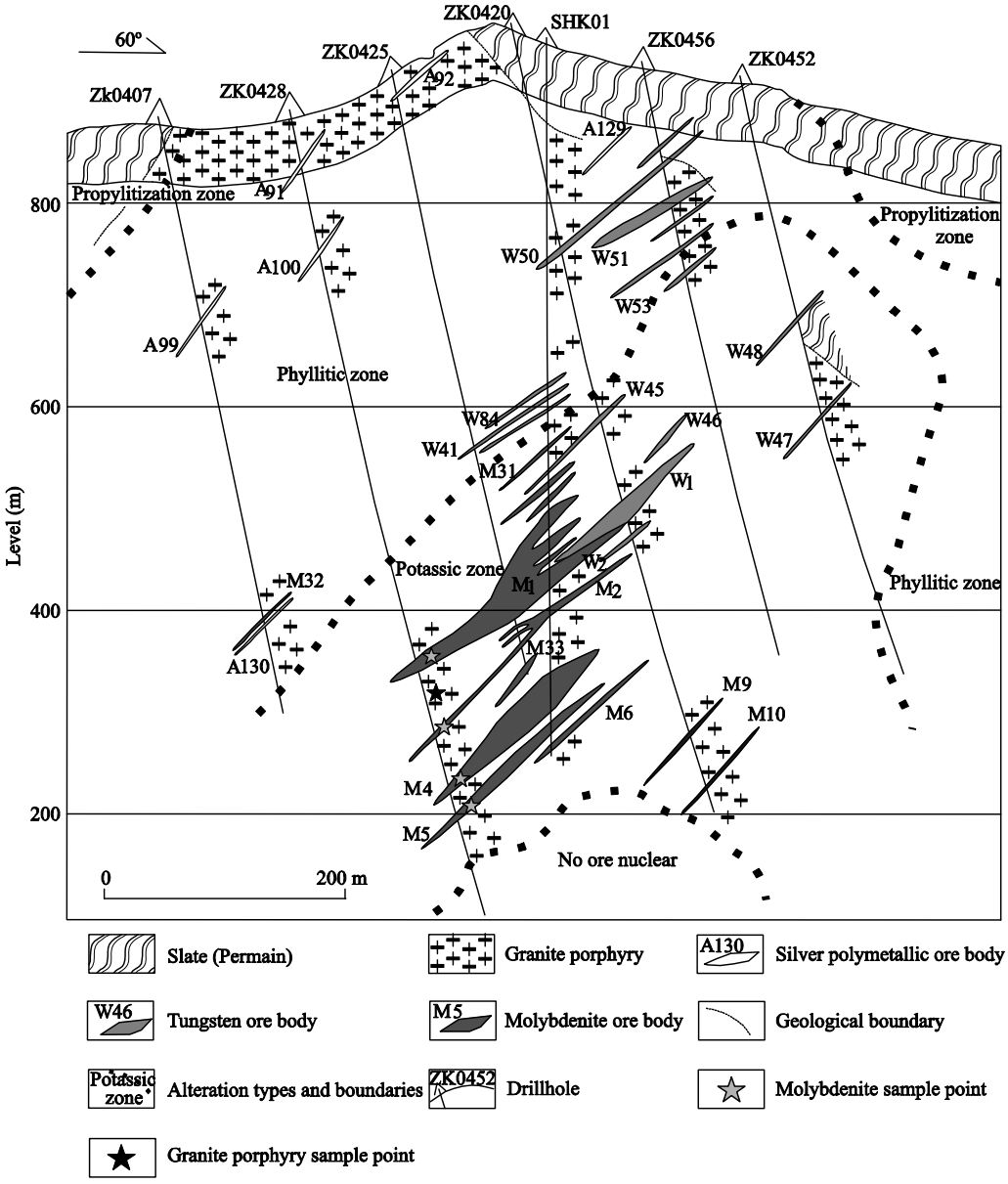

Figure 4. Geological section of exploration Line 04 in ore block I in the Mo-W polymetallic ore deposit.

ore-forming elements are zoned and mainly present Mo, W, and Ag polymetallic mineralization zones (Li et al., 2010).

Based on the mineral assemblages and crosscuting relationships, the mineral paragenesis is divided into three stages: wolframite±cassiterite±arsenopyrite-quartz (Stage I), arsenopyrite±molybdenite-quartz (Stage II), and silver- polymetallic sulfides-quartz (Stage III) (Fig. 5). The W and Sn mineralization mainly formed in Stage I, the Mo mineralization primarily occurred during Stage II, and the silver-polymetallic ores mainly appeared in Stage III.

2 ANALYTICAL METHODS

2.1 Zircon U-Pb Dating

Zircon U-Pb ages were determined for sample ZK0428 from the Dongshanwan deposit (Fig. 4). The sample was crushed, and zircon grains were separated at the Hebei Institute of Geological Surveying and Mapping, Langfang, China. Cathodoluminescence (CL) images and isotopic analyses of the zircons were performed at the State Key Laboratory of Geological Processes and Mineral Resources, China University of Geosciences, Wuhan, China. The zircon grains were mounted in epoxy blocks and polished to expose the grain centers. The CL images were obtained using an optical microscope and a JEOL scanning electron microscope. U-Pb dating and trace element analyses of zircons were obtained using an Agilent 7500a ICP-MS and GeoLas 2005 laser ablation system. $^{206}Pb/^{238}U$ ratios were calculated by ICPMSDataCal (Liu Y S et al., 2010, 2008), while the concordia age diagram and probability density plots of detrital zircon were obtained with Isoplot 3.0 (Ludwig, 2003). An Agilent 7500a ICP-MS was used to acquire ion signal intensities, and helium was used as the carrier gas. Argon was used as the make-up gas and was mixed with the carrier gas via a T-connector before entering the ICP. Nitrogen was added to the central flow of Ar+He, and Ar plasma was used to reduce the detection limit and improve precision (Hu et al., 2008).

2.2 Re-Os Isotope Analyses

Zircon U-Pb for 5 samples of veinlet-disseminated molybdenite were collected from different depths in drillcore ZK0428 (Fig. 4). The Re-Os isotope analyses were performed at the Re-Os Laboratory, National Research Center of Geoanalysis, Chinese Academy of Geological Sciences, Beijing, China. Separation of Os by distillation and extraction of Re were performed following Du et al. (2007, 1994). Uncertainties in the concentrations of Re and Os include those due to errors in the weighing of sample and diluent, calibration errors of the diluent, fractionation correction errors of the mass spectrometry measurements, and isotopic ratio measurement errors of the test sample. Values are reported with 95% confidence levels. The Re-Os model ages were calculated as $t=[\ln(1+^{187}Os/^{187}Re)]/\lambda$, where λ is the decay constant of ^{187}Re (1.666×10^{-11}/year) (Smoliar et al., 1996).

2.3 Major and Trace Elements

Major, trace, and rare earth elements were measured at the State Key Laboratory of Geological Processes and Mineral Resources, China University of Geosciences, Wuhan, China. The samples were crushed in a steel jaw crusher and then powdered to 200 meshes in an agate mill. Major element compositions were analyzed by X-ray fluorescence (Magix-pro 2440), with analytical uncertainties of 5%. Rare earth element compositions were analyzed using an Agilent 7500a ICP-MS; the precision and accuracy of major elements was better than 5% (Liu Y S et al., 2010, 2008).

3 RESULTS

3.1 Zircon U-Pb Age

Most of the zircons from the granite porphyry in the Dongshanwan ore district exhibit oscillatory or planar zoning under CL, as are typical of magmatic zircons (Fig. 6). The results of U-Pb dating of 20 zircons are listed in Table 1. The Th/U ratios range from 0.3 to 1.07, indicating a magmatic origin of the zircons (Hoskin and Black, 2000); 17 of the zircons analyses are near the concordia curve (Fig. 7). The $^{206}Pb/^{238}U$ ages range from 141±2 to 144±3 Ma, with a mean of 142.15±0.91 Ma (MSWD=0.58), which represents the crystallization age of the granite porphyry. Two measured points deviate from the concordia curve, and the $^{206}Pb/^{238}U$ age of the remaining zircon is 352 Ma. These three ages are interpreted as the crystallization ages of zircons captured or entrained from the wall rock during ascent of the magma.

3.2 Molybdenite Re-Os Age

The Re-Os isotopic compositions of five molybdenite samples from the Dongshanwan deposit are listed in Table 2. Model ages for these samples range from 139.9 to 141.5 Ma, with a weighted mean age of 140.4±1.8 Ma. The samples yield an isochron age of 140.5±3.2 Ma (MSWD=1.2) (Fig. 8), which indicates the timing of mineralization, and this age is close to the crystallization age of the ore-bearing granite porphyry.

3.3 Geochemistry of the Granite Porphyry

The major elements for granite porphyry are presented in Table 3. Chemical analyses show high SiO_2 (75.25 wt.%–76.26 wt.%), relatively low Al_2O_3 values, and high alkali compositions (K_2O+Na_2O, 8.19 wt.%–9.45 wt.%). The Rittmann index (σ) varies from 2.07 to 2.77, as shown on a SiO_2 vs. K_2O diagram (Fig. 9a), and all samples plotted in the high-K calc-alkaline series field. The A/CNK values range from 0.87 to 1.02 and plotted in the peralkaline field on an A/CNK vs. A/NK diagram (Fig. 9b).

Rare earth elements for the Dongshanwan samples are listed in Table 4. The Dongshanwan samples show a narrow range of ΣREE values (158 ppm–186 ppm), LREE values from 120.55

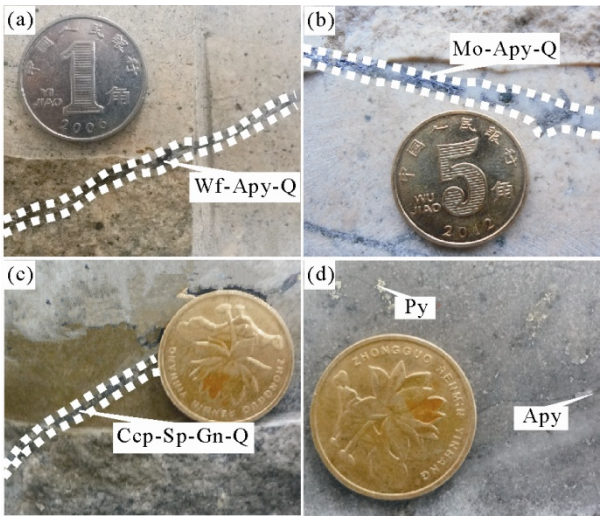

Figure 5. Photographs of ore veins in the Dongshanwan deposit. (a) Wolframite-(cassiterite)-arsenopyrite-quartz vein; (b) arsenopyrite-molybdenite-quartz vein; (c) chalcopyrite-galena-sphalerite-quartz vein; (d) disseminated minerals. Wf. Wolframite; Mo. molybde; Ccp. cassiterite; Sp. sphalerite; Gn. galena; Q. quartz; Py. pyrite; Apy. arsenopyrite.

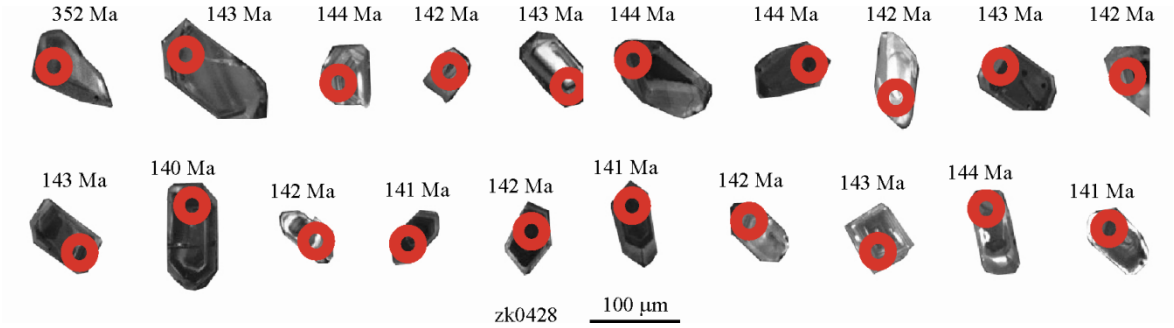

Figure 6. Cathodoluminescence images of zircons from granite porphyry in the Dongshanwan deposit.

Table 1 LA-ICP-MS U-Pb data of zircons from the granite porphyry in the Dongshanwan deposits

Spot No.	Concentration (ppm)		Th/U	Isotopic ratios									
				$^{207}Pb/^{206}Pb$		$^{207}Pb/^{235}U$		$^{206}Pb/^{238}U$		$^{207}Pb/^{235}U$		$^{206}Pb/^{238}U$	
	^{232}Th	^{238}U		Ratio	1σ	Ratio	1σ	Ratio	1σ	Age (Ma)	1σ	Age (Ma)	1σ
ZK0428-1	347.8	819.4	0.42	0.053 20	0.001 67	0.416 38	0.014 67	0.056 14	0.001 14	353	11	352	7
ZK0428-2	2 122.2	1 987.7	1.07	0.049 88	0.001 71	0.156 04	0.005 27	0.022 47	0.000 23	147	5	143	1
ZK0428-3	445.3	844.8	0.53	0.050 05	0.002 01	0.156 22	0.006 14	0.022 64	0.000 30	147	5	144	2
ZK0428-4	539.2	999.9	0.54	0.047 31	0.003 72	0.147 00	0.013 23	0.022 27	0.000 84	139	12	142	5
ZK0428-5	932.6	1 382.4	0.67	0.052 83	0.002 28	0.163 44	0.006 74	0.022 42	0.000 30	154	6	143	2
ZK0428-6	1 843.3	2 089.1	0.88	0.051 79	0.001 84	0.162 36	0.005 77	0.022 55	0.000 27	153	5	144	2
ZK0428-7	2 132.0	2 347.1	0.91	0.052 67	0.002 91	0.164 81	0.008 75	0.022 54	0.000 32	155	8	144	2
ZK0428-8	120.9	399.6	0.30	0.052 84	0.007 19	0.163 90	0.022 14	0.022 30	0.000 91	154	19	142	6
ZK0428-9	2 857.0	5 273.0	0.54	0.050 05	0.002 11	0.157 62	0.008 12	0.022 48	0.000 47	149	7	143	3
ZK0428-10	1 821.2	2 173.0	0.84	0.051 26	0.004 61	0.158 21	0.010 86	0.022 22	0.001 00	149	10	142	6
ZK0428-11	1 246.5	1 583.7	0.79	0.042 82	0.014 24	0.152 81	0.047 19	0.022 45	0.000 98	144	42	143	6
ZK0428-12	1 578.9	2 320.4	0.68	0.052 41	0.001 97	0.161 50	0.005 66	0.022 20	0.000 25	152	5	142	2
ZK0428-13	633.7	944.6	0.67	0.046 65	0.002 84	0.144 87	0.008 91	0.022 28	0.000 38	137	8	142	2
ZK0428-14	219.9	588.4	0.37	0.045 54	0.008 00	0.142 07	0.027 53	0.022 14	0.000 64	135	24	141	4
ZK0428-15	2 104.1	2 088.1	1.01	0.051 53	0.003 54	0.158 80	0.010 49	0.022 29	0.000 39	150	9	142	2
ZK0428-16	282.3	752.4	0.38	0.051 39	0.002 95	0.158 75	0.009 29	0.022 15	0.000 30	150	8	141	2
ZK0428-17	291.4	777.3	0.37	0.053 07	0.002 91	0.163 66	0.008 71	0.022 35	0.000 31	154	8	142	2
ZK0428-18	495.2	706.5	0.70	0.054 00	0.003 92	0.164 59	0.010 87	0.022 36	0.000 55	155	9	143	3
ZK0428-19	936.1	1 400.2	0.67	0.050 85	0.004 00	0.160 26	0.012 34	0.022 62	0.000 44	151	11	144	3
ZK0428-20	947.0	1 175.1	0.81	0.045 58	0.002 65	0.139 67	0.007 88	0.022 07	0.000 34	133	7	141	2

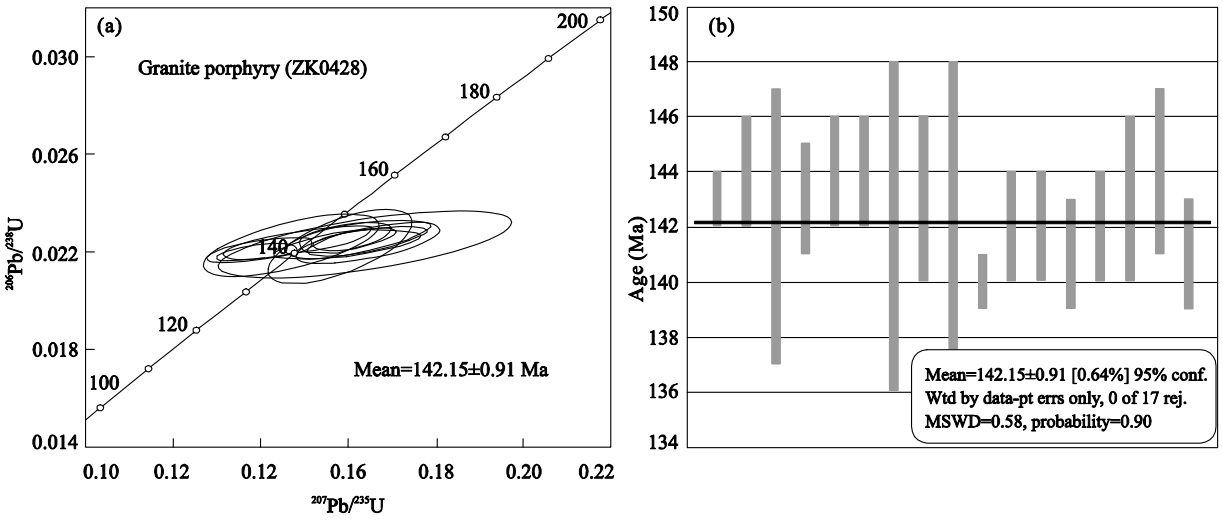

Figure 7. Zircon concordia diagram (a) and weighting diagram (b) for granite porphyry in the Dongshanwan deposits.

Table 2 Re-Os isotopes of molybdenite from the Dongshanwan deposit

		Re (ng/g)		Os (ng/g)		Re^{187} (ng/g)		Os^{187} (ng/g)		Model ages (Ma)	
Sample No.	Weight (g)	Measured	2σ	Measured	2σ	Measured	2σ	Measured	2σ	Measured	2σ
Mo-1	0.060 16	224.72	0.69	0.012 8	0.001 1	141.12	0.44	0.331 2	0.002 7	140.0	2.0
Mo-2	0.055 44	72.62	0.24	0.003 3	0.000 4	45.64	0.15	0.107 3	0.000 6	141.0	1.7
Mo-3	0.063 15	234.48	0.68	0.002 1	0.000 3	147.79	0.42	0.347 2	0.006 9	141.5	3.1
Mo-4	0.072 12	94.95	0.33	0.003 5	0.001 7	60.68	0.21	0.139 2	0.001 7	139.9	2.3
Mo-5	0.056 49	121.02	0.39	0.004 5	0.002 2	75.07	0.24	0.177 5	0.002 2	139.9	1.9

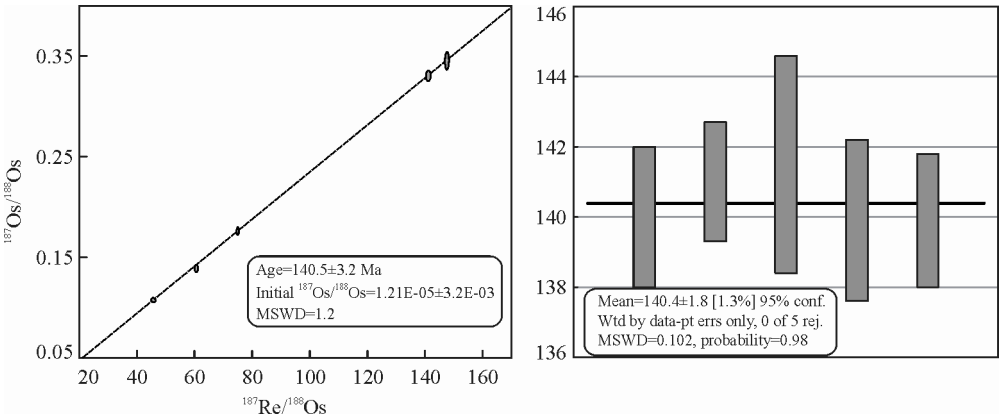

Figure 8. Re-Os isochrons and model ages for molybdenite samples from the Dongshanwan deposits.

Table 3 Major element (wt.%) compositions and zircon saturation temperature of the granite porphyry in Dongshanwan

Samples	SiO_2	TiO_2	Al_2O_3	Fe_2O_3	MnO	MgO	CaO	Na_2O	K_2O	P_2O_5	LOI	Total	Zr-T (ºC)
DSW-1	75.45	0.06	12.33	1.06	0.02	0.12	0.38	4.08	4.46	0.01	0.37	98.33	819
DSW-2	75.39	0.09	12.09	1.33	0.05	0.08	0.41	4.46	3.73	0.01	0.17	97.79	825
DSW-3	76.15	0.08	12.27	1.21	0.02	0.09	0.44	3.87	4.53	0.01	0.69	99.35	823
DSW-4	75.25	0.088	11.95	1.21	0.02	0.08	0.48	4.61	4.84	0.018	0.68	99.27	811
DSW-5	76.52	0.086	11.52	1.51	0.02	0.09	0.43	3.92	4.69	0.018	0.69	98.87	822

Table 4 Trace element and rare earth element compositions (ppm) of the granite porphyry in Dongshanwan

Sample	DSW-1	DSW-2	DSW-3	DSW-4	DSW-5	Sample	DSW-1	DSW-2	DSW-3	DSW-4	DSW-5
La	19.6	26.9	21.2	15.3	30.7	δEu	0.006	0.009	0.007	0.005	0.010
Ce	52.8	68.6	62.5	57.6	63.3	Rb	229	217	223	249	200
Pr	7.26	8.95	8.12	5.60	10.26	Ba	11.7	8.31	10.9	12.80	9.2
Nd	31.5	35.7	33.8	34.3	32.9	Th	22.4	23.4	22.8	24.5	21.6
Sm	9.35	9.46	9.41	10.20	8.73	U	8.08	8.68	8.34	8.82	8.01
Eu	0.018	0.026	0.022	0.016	0.031	Ta	1.33	1.52	1.41	1.45	1.40
Gd	9.31	8.92	9.14	7.24	10.19	Nb	12.2	13.4	12.9	13.4	14.2
Tb	1.65	1.61	1.63	1.28	1.84	Sr	6.96	7.69	7.31	7.80	7.32
Dy	10.4	9.97	10.2	8.10	11.4	Zr	137	148	142	140	145
Ho	2.09	1.97	2.03	1.62	2.26	Hf	6.20	6.86	6.61	6.77	6.33
Er	6.15	6.04	6.09	4.79	6.90	Sm	9.35	9.46	9.41	10.20	8.73
Tm	0.91	0.94	0.93	0.72	1.07	Ti	360	540.0	480.0	392.0	498.4
Yb	5.96	6.06	6.01	6.50	5.60	Y	60.4	59.6	60.1	65.9	55.0
Lu	0.89	0.91	0.90	0.97	0.84	Ga	23.3	22.8	23.1	21.2	24.1
Be	6.16	5.73	5.98	6.23	5.68	Rb/Sr	32.85	28.19	30.51	31.92	27.32
ΣREE	157.9	186.0	174.1	160.3	180.1	Nb/Ta	9.23	8.86	9.15	9.24	10.14
LaN/YbN	2.36	3.18	2.79	2.36	3.18	Zr/Y	2.27	2.49	2.36	2.12	2.64

ppm to 149.58 ppm, HREE values from 31.19 ppm to 40.08 ppm, LREE/HREE ratios from 3.23 to 4.14, and $(La/Yb)_N$ values from 2.36 to 3.18. The samples are enriched in LREEs. The δEu values of 0.005–0.010 indicate significant Eu depletion (Fig. 10a). A clear negative Eu anomaly indicates that the source region for the granite contained a large amount of plagioclase or those plagioclase fractionated from the magmas (Hassanen, 1997).

Trace elements are given in Table 4 and plotted on a primitive-mantle-normalized trace element diagram in Fig. 10b. The samples are enriched in incompatible elements (e.g., Zr, Hf, and Y) and some large ion lithophile elements (LILE; e.g., Ba, Sr, and K), whereas high field strength elements (HFSE; e.g., Ti, Nb, and P) show negative anomalies. Depletions in P and Ti may indicate that these rocks underwent fractional crystallization of apatite and ilmenite (Miller et al., 1999), and negative Sr and Ba anomalies indicate that plagioclase separation has occurred.

Generally, the granite porphyry of Dongshanwan is A-type granites, which is characteristically enriched in SiO_2 and alkalis, depleted in Al_2O_3, shows Ti, Ba, and P anomalies, has Sr values of <10 ppm, and possess clear negative Eu anomalies (Zhang et al., 2012).

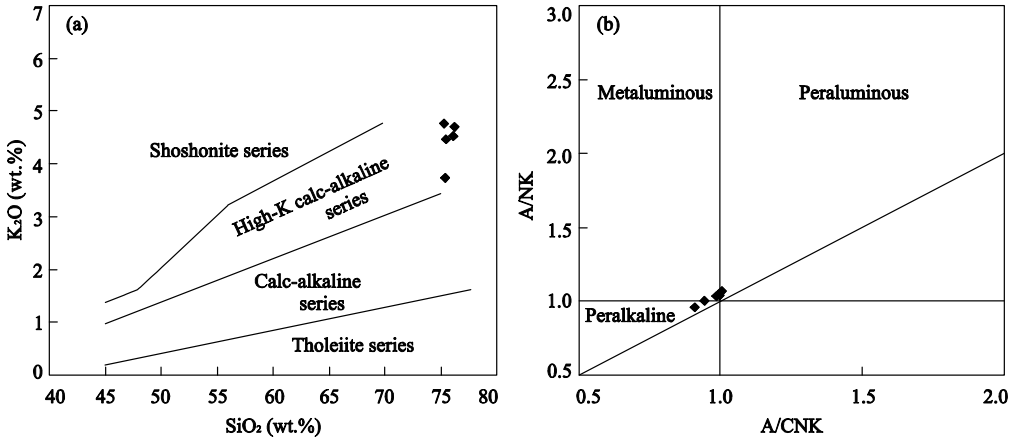

Figure 9. (a) SiO_2 vs. K_2O diagram (after Rickwood, 1989) and (b) an A/CNK vs. A/NK diagram (after Peccerillo and Taylor, 1976).

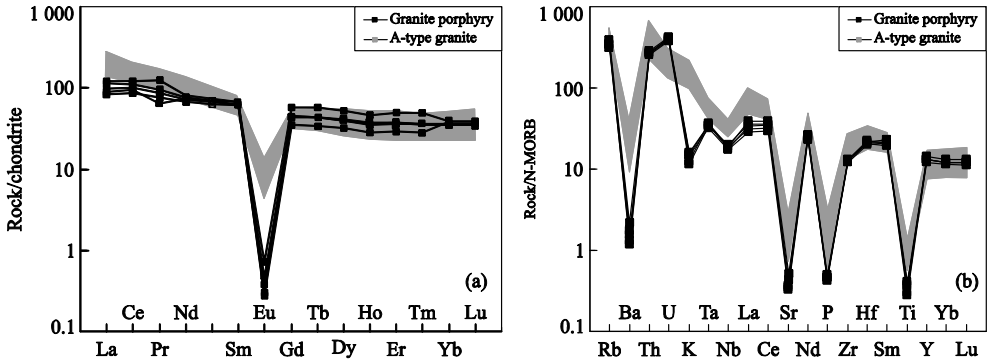

Figure 10. (a) Chondrite-normalized REE pattern of granite porphyry in the Dongshanwan deposit and (b) a primitive-mantle-normalized spider diagram of granite porphyry in the Dongshanwan deposit. Chondrite normalizing values are after Sun and McDonough (1989) (data in the gray band are from Zhang et al., 2007).

4 DISCUSSION

4.1 Formation and Timing of Mineralization of the Granite Porphyry

The U-Pb dating gives a crystallization age for the granite porphyry of 142.15±0.91 Ma, and the Re-Os isotopic analyses gives a molybdenite mineralization age of 140.5±0.32 Ma. Similar ages of host intrusion and mineralization indicate that mineralization was closely associated with magmatic hydrothermal fluids in the granite porphyry. Moreover, mineralization in the Xilamulun molybdenum metallogenic belt is related to granitic magmatism, suggesting a genetic link between the molybdenum mineralization and the granitic rocks. The Early Cretaceous (145–130 Ma) was a time of significant Mo mineralization in the Xilamulun metallogenic belt on the northern margin of the North China Craton (Zhu et al., 2016; Zeng et al., 2014, 2013, 2012, 2011, 2010a, b; Liu J M et al., 2010; Ma et al., 2009; Nie et al., 2007).

4.2 Source of Ore-Forming Materials

Mao et al. (1999) reported that the sources of ore-forming materials can be identified from the Re values of molybdenite, decreasing exponentially from mantle ($n\times10^{-4}$) to mixed crust-mantle ($n\times10^{-5}$) and crustal sources ($n\times10^{-6}$). Molybdenite from the Dongshanwan Mo-W deposit displays low Re contents ranging from 0.07 ppm to 0.22 ppm, indicating a crustal source for the ore-forming materials. What's more, the granite porphyry is the ore-forming intrusion of the Dongshanwan Mo-W deposit, therefore, certainly Mo-W was sourced from the granite porphyry. The high SiO_2, and low MgO and TFe_2O_3 concentrations of the Dongshanwan granite porphyry, combined with its high-K calc-alkaline characteristics, LILE and LREE enrichment, and HFSE depletion, suggest that the primary magma was derived from the partial melting of crustal material (Xu et al., 2009). Furthermore, Zeng et al. (2015) reported the Hf isotope composition Dongshanwan granite porphyry, suggesting that primary magma was derived from a very juvenile crust-derived magma source with some composition of the depleted mantle. Combined with the discussions above, it can be speculated that the ore-forming materials of the Dongshanwan Mo-W deposit may be brought by the granite porphyry mainly from juvenile crustal source.

4.3 Petrogenetic Type for Granite Porphyry

Dongshanwan granite porphyry is high SiO_2, alkalis, and low Al_2O_3, and shows Ti, Ba, and P anomalies, exhibiting a low Sr values, and possesses clear negative Eu anomalies. On the Zr, Nb, Ce, $(Na_2O+K_2O)/CaO$ vs. 10 000Ga/Al diagrams (Figs. 11a–11d), all samples of the granite porphyry and coeval intrusions in the region plotted in the A-type granite field. Dongshanwan granite porphyry has the chemical characteristics of A-type granites, which is characteristically enriched in SiO_2 and K_2O, shows Ba and Sr anomalies, and exhibits clearly

negative Eu anomalies (Zhang et al., 2012; Wu et al., 2002). Moreover, we calculate the Zr saturation temperature of the Dongshanwan granite porphyry, it shows high-temperature nature (811 to 825 ºC, calculated by the equation from Watson and Harrison (1983)), which suggests that Dongshanwan granite porphyry is A-type granite and does not belong to high fractionated I type granite (Wu et al., 2007; King et al., 2001, 1997). On Nb-Y-Ce and Nb-Y-3Ga diagrams (Figs. 11e, 11f), samples of the granite porphyry predominantly plotted in the A2-type granite field. Eby (1992, 1990) proposed that A2-type granites are derived from continental crust or island arc basalts that formed in a post- collisional or post-orogenic tectonic setting.

4.4 Tectonic Setting

During the Paleozoic, the region of southern Great Xing'an Range saw the evolution and closure of the Paleo-Asian Ocean. In the Mesozoic, the Great Xing'an Range was overprinted by the circum-Pacific tectonic regime and the Mongol-Okhotsk tectonic regime. Three models have been proposed for the tectonic setting of the southern segment the Great Xing'an Range in the Mesozoic. (1) The Triassic–Jurassic granitoids and the Early Mesozoic porphyry Cu-Mo ore deposits in the southern segment of the Great Xing'an Range were related to the evolution of the Mongol-Okhotsk tectonic regime (Zeng et al., 2014, 2012, 2011; Wu G et al., 2008; Mao et al., 2005; Wang et al., 2002). (2) The formation of the Mesozoic volcanics and granitoids in the Great Xing'an Range were related to the subduction of the Paleo-Pacific Plate beneath the Eurasian continent (Liu et al., 2015; Zeng et al., 2011; Zhou et al., 2010; Wakita and Metcalfe, 2005; Wu et al., 2000). (3) The deposits of the Great Xing'an Range were influenced by both the Mongol-Okhotsk tectonic regime and the subduction of the Paleo-Pacific Plate regime (Zhang L C et al., 2010).

Whether the mineralization of Early Cretaceous in the Xilamulun metallogenic belt were influenced by the subduction and collision of the Mongol-Okhotsk tectonic regime can be clearly recognized by the following facts: (1) Volcanic rocks of the Great Xing'an Range are typical A-type rhyolites, indicating that the region was situated in extensional environment at the time of eruption of these rocks (Wang et al., 2013; Meng et al., 2011; Gou et al., 2010). In addition, the Late Jurassic and early Early Cretaceous intrusions and volcanic rocks are classified mainly as alkaline series and/or bimodal volcanic rocks, suggesting that they formed in an extensional environment (Meng et al., 2011; Xu et al., 2011; Zhang J H et al., 2008; Wang et al., 2006). The lack of calc-alkaline igneous rocks within these Late Jurassic and early Early Cretaceous igneous rocks also argue against their formation occurred in a subduction-related tectonic setting, as well. (2) Kravchinsky et al. (2002) proposed that the Mongol-Okhotsk Ocean closed in the Jurassic, that the Great Xing'an Range is a result of the thickening of continental crust after the closure of the Mongol-Okhotsk Ocean (Zhao Y et al., 1994), and that the southern Great Xing'an Range was in an extensional environment during 135–150 Ma, influenced by the collapse or delamination of thickened continental crust (Xu et al., 2013; Bai et al., 2012; Meng, 2003). (3) The unconformity of volcanic rocks in Jibei and Liaoxi on the Tuchengzi Formation and in the Upper Tuchengzi Formation represents the southward movement of thrust nappes (Zhang Y Q et al., 2008), which may be related to collapse or delamination of thickened continental crust after the closure of the Mongol-Okhotsk Ocean. Therefore, the Dongshanwan Mo-W deposit is possibly related to the evolution of the Mongol-Okhotsk suture belt, rather than to subduction of the Paleo-Pacific Plate beneath the Eurasian continent.

4.5 Insights into Metallogeny

In the Middle–Late Jurassic and Early Cretaceous periods,

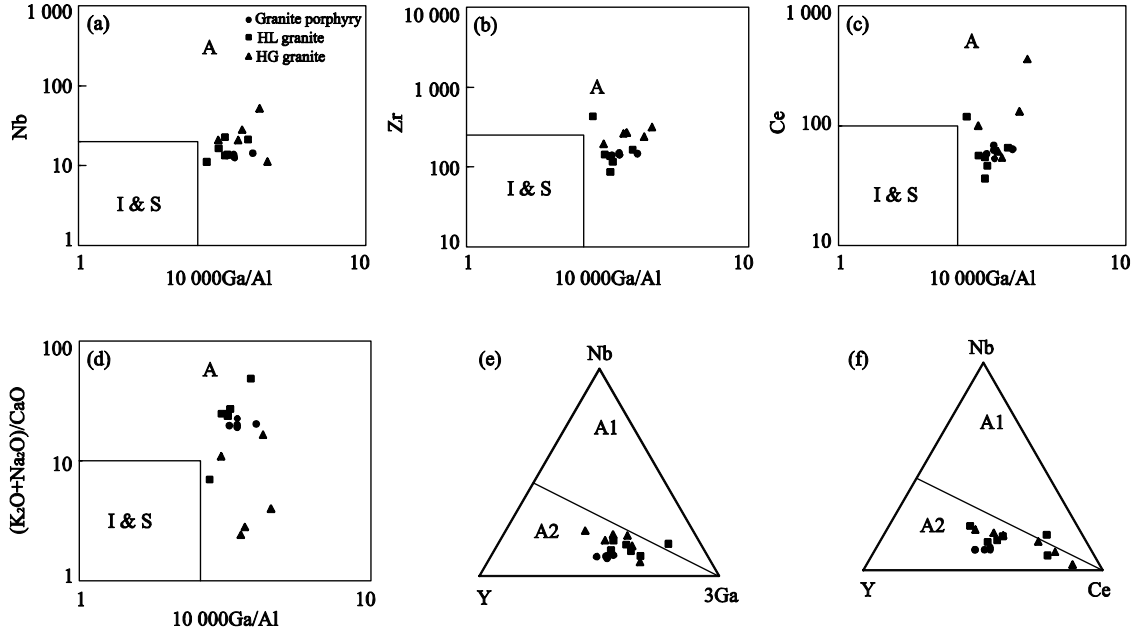

Figure 11. (a) Nb vs. 10 000Ga/Al, (b) Zr vs. 10 000Ga/Al, (c) Ce vs. 10 000Ga/Al, (d) (Na_2O+K_2O)/CaO vs. 10 000Ga/Al (after Whalen et al., 1987), (e) Nb-Y-3Ga, and (f) Nb-Y-Ce (after Eby, 1992) (HL granite and HG data are from Li, 2014; Zhou et al., 2010). HL. Hongling; HG. Huanggang.

the Mongol-Okhotsk tectonic regime led to the collapse or delamination of the thickening continental crust in the Xilamulun metallogenic belt (Xu et al., 2013; Zhang J H et al., 2008; Zhao et al., 1994). The porphyry-type deposits can occur in an extensional setting, and porphyry ore-forming system generates in stress release period of post-collision or transition stage of structure regime (Sillitoe, 2010; Hou et al., 2009; Richards, 2009; Hou, 2004). Because of mantle thinning or slab break-off in extensional setting, the upwelling of asthenosphere has probably provided either enough heat to cause partial melting of thickened lower crustal source rocks, or contributed a significant juvenile component (including Cu and Mo) into a lower crustal source (Hou et al., 2003). The regional extension setting in the Late Jurassic and Early Cretaceous formed the significant Mo mineralization (e.g., Jiguanshan, Xiaodonggou, Banlashan, Aolunhua, etc.) in the Xilamulun metallogenic belt, these deposits have a genetic relation with the collapse or delamination of the thickened continental crust. According to the mineralization age, the Dongshanwan deposit formed in an extensional environment during the Early Cretaceous. During the collapse or delamination of the thickened crust, intermediate-acidic magma, mixed with depleted mantle material, intruded the Zhesi Formation and formed the Dongshanwan granite porphyry in the period of cooling, and further formed the Mo polymetallic mineralization.

5 CONCLUSIONS

(1) The Dongshanwan Wu-Mo polymetallic deposit is a porphyry-type deposit. An analysis of mineral assemblages indicates that mineralization occurred in three stages: (i) wolframite±cassiterite±arsenopyrite-quartz (Stage I), (ii) arsenopyrite±molybdenite-quartz (Stage II), and (iii) silver-polymetallic sulfide-quartz stage (Stage III).

(2) LA-ICP-MS U-Pb zircon dating indicates that the granite porphyry of the Dongshanwan deposit crystallized at 142.15±0.91 Ma. The granite porphyry is A2-type granite and formed in a post-orogenic extensional environment.

(3) Re-Os isotope analyses yield an age of 140.5±3.2 Ma for molybdenite mineralization, indicating that ore formation in the Dongshanwan deposit was associated with Early Cretaceous magmatism. The Re values of molybdenite and geochemical data of granite porphyry indicate crustal source materials for the Dongshanwan deposit.

(4) The Early Cretaceous Mo mineralization in the Xilamulun metallogenic belt may be related to post-collisional extension of the Mongol-Okhotsk suture belt, and those deposits have a genetic relation with the collapse or delamination of the thickened continental crust.

ACKNOWLEDGMENTS

This study was supported by the Opening Foundation of the State Key Laboratory of Geological Processes and Mineral Resources, China University of Geosciences (No. GPMR201307). The authors are most grateful to the staff of the State Key Laboratory of Geological Processes and Mineral Resources (China University of Geosciences, Wuhan) as well as the Institute of Geology and Geophysics, Chinese Academy of Sciences during the zircon U-Pb dating, geochemical analyses and Re-Os isotopic analyses. The final publication is available at Springer via http://dx.doi.10.1007/s12583-016-0934-1.

REFERENCES CITED

Bai, L. A., Sun, J. G., Zhang, Y., et al., 2012. Genetic Type, Miner-Alization Epoch and Geodynamical Setting of Endogenous Copper Deposits in the Great Xing'an Range. *Acta Petrologica Sinica*, 28(2): 468–482 (in Chinese with English Abstract)

Chen, Z. G., Ghang, L. C., Wu, H. Y., et al., 2008. Geochemistry Study and Tectonic Background of A Style Host Granite in Nianzigou Molybdenum Deposit in Xilamulun Molybdenum Deposit in Xilamulun Molybdenum Metallogenic Belt, Inner Mongolia. *Acta Petrologica Sinica*, 24(4): 879–889 (in Chinese with English Abstract)

Ding, Q. F., Yan, W., Zhang, B. L., 2016. Sulfur- and Lead-Isotope Geochemistry of the Balugou Cu-Pb-Zn Skarn Deposit in the Wulonggou Area in the Eastern Kunlun Orogen, NW China. *Journal of Earth Science*, 27(5): 740–750

Du, A. D., He, H. L., Yin, N. W., 1994. A Study of the Rheniumosmium Geochronometry of Molybdenites. *Acta Geologica Sinica*, 8(2): 171–181 (in Chinese with English Abstract)

Du, A. D., Qu, W. J., Wang, D. H., et al., 2007. Subgrain-Size Decoupling of Re and ^{187}Os with in Molybdenite. *Mineral Deposits*, 26(5): 572–580 (in Chinese with English Abstract)

Duan, X. X., Zeng, Q. D., Yang, Y. H., et al., 2015. Triassic Magmatism and Mo Mineralization in Northeast China: Geochronological and Isotopic Constraints from the Laojiagou Porphyry Mo Deposit. *International Geology Review*, 57(1): 55–75. doi:10.1080/00206814.2014.989546

Eby, G. N., 1990. The A-Type Granitoids: A Review of Their Occurrence and Chemical Characteristics and Speculations on Their Petrogenesis. *Lithos*, 26(1/2): 115–134. doi:10.1016/0024-4937(90)90043-z

Eby, G. N., 1992. Chemical Subdivision of the A-Type Granitoids: Petrogenetic and Tectonic Implications. *Geology*, 20(7): 641–644. doi:10.1130/0091-7613(1992)020<0641:csotat>2.3.co;2

Fu, Z. R., Chen, H. J., 2004. Geological Characteristics and Prospect of Mineral Exploration of Dongshanwan W-Sn-Be Deposit at Balinzuo County of Inner Mongolia. *Journal of Guilin Institute of Technology*, 24(2): 148–151 (in Chinese with English Abstract)

Gou, J., Sun, D. Y., Zhao, Z. H., et al., 2010. Zircon LA-ICP MS U-Pb Dating and Petrogenesis of Rhyolites in Baiyingaolao Formation from the Southern Manzhouli, Inner-Mongolia. *Acta Petrologica Sinica*, 25(1): 333–344 (in Chinese with English Abstract)

Hassanen, M. A., 1997. Post-Collision, A-Type Granites of Homrit Waggat Complex, Egypt: Petrological and Geochemical Constraints on Its Origin. *Precambrian Research*, 82(3): 211–236. doi:10.1016/s0301-9268(96)00042-3

Hoskin, P. W. O., Black, L. P., 2000. Metamorphic Zircon Formation by Solid-State Recrystallization of Protolith Igneous Zircon. *Journal of Metamorphic Geology*, 18(4): 423–439. doi:10.1046/j.1525-1314.2000.00266.x

Hou, Z. Q., 2004. Porphyry Cu-Mo-Au Deposits: Some New Insights and Advances. *Earth Science Frontiers*, 1(3): 131–144

Hou, Z. Q., Mo, X. X., Gao, Y. F., et al., 2003. Adakite, A Possible Host Rock for Porphyry Copper Deposits: Case Studies of Porphyry Copper Belts in Tibetan Plateau and in Northern Chile. *Mineral Deposits*, 22(1): 1–12 (in Chinese with English Abstract)

Hou, Z. Q., Yang, Z. M., Qu, X. M., et al., 2009. The Miocene Gangdese Porphyry Copper Belt Generated during Post-Collisional Extension in the Tibetan Orogen. *Ore Geology Reviews*, 36(1): 25–51.

doi:10.1016/j.oregeorev.2008.09.006

Hu, Z. C., Gao, S., Liu, Y., et al., 2008. Signal Enhancement in Laser Ablation ICP-MS by Aaddition of Nitrogen in the Central Channel Gas. *Journal of Analytical Atomic Spectrometry*, 23(8): 1093–1101 (in Chinese with English Abstract)

Jahn, B. M., Wu, F. Y., Chen, B., 2000. Granitoids of the Central Asian Orogenic Belt and Continental Growth in the Phanerozoic. *Geological Society of America Special Papers*, 350(1/2): 181–193. doi:10.1017/s0263593300007367

King, P. L., Chappell, B. W., Allen, C. M., et al., 2001. Are A-Type Granites the High-Temperature Felsic Granites? Evidence from Fractionated Granites of the Wangrah Suite. *Australian Journal of Earth Sciences*, 48(4): 501–514. doi:10.1046/j.1440-0952.2001.00881.x

King, P. L., White, A. J. R., Chappell, B. W., et al., 1997. Characterization and Origin of Aluminous A-Type Granites from the Lachlan Fold Belt, Southeastern Australia. *Journal of Petrology*, 38(3): 371–391. doi:10.1093/petroj/38.3.371

Kravchinsky, V. A., Cogné, J. P., Harbert, W. P., et al., 2002. Evolution of the Mongol-Okhotsk Ocean as Constrained by New Palaeomagnetic Data from the Mongol-Okhotsk Suture Zone, Siberia. *Geophysical Journal International*, 148(1): 34–57. doi:10.1046/j.1365-246x.2002.01557.x

Li, J. F., 2014. Mineralization and Periphery Metallogenic Prediction of the Hongling Pb-Zn Polymetallic Deposit in Chifeng, Inner Mongolia: [Dissertation]. Jilin University, Changchun. 100–103 (in Chinese with English Abstract)

Li, J. Y., Mo, S. G., He, Z. J., 2004. The Timing of Crustal Sinistral Strike-Slip Movement in the Northern Great Khing'an Ranges and Its Constraint on Reconstruction of the Crustal Tectonic Evolution of NE China and Adjacent Areas since the Mesozoic. *Earth Science Frontiers* 172(3–4): 223–249

Li, Z. M., Huang, H. L., Zhang, Z., et al., 2010. The Exploration Report of the Dongshanwan Polymetal Deposit in Balinzuoqi, Inner Mogolia. No. 243 Geological Team, National Nuclear Industry Geology Bureau, Chifeng. 1–57 (in Chinese)

Liu, J. L., Sun, F. Y., Lin, B. L., et al., 2015. Geochronology, Geochemistry and Zircon Hf Isotope of Miantian Granodiorite Intrusion in Yanbian Region, Southern-Jinlin Province and Its Geological Significance. *Earth Science—Journal of China University of Geosciences*, 40(1): 49–60

Liu, J. M., Zhao, Y., Sun, Y. L., et al., 2010. Recognition of the Latest Permian to Early Triassic Cu-Mo Mineralization on the Northern Margin of the North China Block and Its Geological Significance. *Gondwana Research*, 17(1): 125–134. doi:10.1016/j.gr.2009.07.007

Liu, Y. S., Hu, Z. C., Gao, S., et al., 2008. In Situ Analysis of Major and Trace Elements of Anhydrous Minerals by LA-ICP-MS without Applying an Internal Standard. *Chemical Geology*, 257(1): 34–43. doi:10.1016/j.chemgeo.2008.08.004

Liu, Y. S., Hu, Z. C., Zong, K. Q., et al., 2010. Reappraisement and Refinement of Zircon U-Pb Isotope and Trace Element Analyses by LA-ICP-MS. *Chinese Science Bulletin*, 55(15): 1535–1546 (in Chinese)

Lowell, J. D., Guilbert, J. M., 1970. Lateral and Yertical Alteration-Mineralization Zoning in Porphyry Ore Deposits. *Economic Geology*, 65(4): 373–408. doi:10.2113/gsecongeo.65.4.373

Ludwig, K. R., 2003. ISOPLOT 3.0: A Geochronological Toolkit for Microsoft Excel. Berkeley Geochronology Center Special Publication, Berkeley. 1–70

Ma, X. H., Chen, B., Lai, Y., et al., 2009. Petrogenesis and Minerlization Choronology Study on the Aolunhua Porphyry Mo Deposit Inner Mongolia and Its Geological Implications. *Acta Petrologica Sinica*, 25(11): 2939–2950 (in Chinese with English Abstract)

Mao, J. W., Xie, G. Q., Zhang, Z. H., et al., 2005. Mesozoic Largescale Metallogenic Pulses in North China and Corresponding Geodynamic Settings. *Acta Petrologica Sinica*, 21(1): 169–188 (in Chinese with English Abstract)

Mao, J. W., Zhao, Z. C., Zhang, Z. L., et al., 1999. Re-Os Isotopic Dating of Molybdenites in the Xiaoliugou W (Mo) Deposit in the Northern Qilian Mountains and Its Geological Significance. *Geochimica et Cosmochimica Acta*, 63(11): 1815–1818 (in Chinese with English Abstract)

Meng, E., Xu, W. L., Yang, D. B., et al., 2011. Zircon U-Pb Chronology, Geochemistry of Mesozoic Volcanic Rocks from the Lingquan Basin in Manzhouli Area, and Its Tectonic Implications. *Acta Petrologica Sinica*, 27(4): 1209–1226 (in Chinese with English Abstract)

Meng, Q. R., 2003. What Drove Late Mesozoic Extension of the Northern China-Mongolia Tract?. *Tectonophysics*, 369(3): 155–174. doi:10.1016/s0040-1951(03)00195-1

Miller, C., Schuster, R., Klötzli, U., et al., 1999. Post-Collisional Potassic and Ultrapotassic Magmatism in SW Tibet: Geochemical and Sr-Nd-Pb-O Isotopic Constraints for Mantle Source Characteristics and Petrogenesis. *Journal of Petrology*, 40(9): 1399–1424. doi:10.1093/petroj/40.9.1399

Nie, F. J., Zhang, W. Y., Du, A. D., et al., 2007. Re-Os Isotopic Dating on Molybdenite Separates from the Xiaodonggou Porphyry Mo Deposit, Hexigten Qi, Inner Mongolia. *Acta Geologica Sinica*, 81(7): 898–904 (in Chinese with English Abstract)

Peccerillo, A., Taylor, S. R., 1976. Geochemistry of Eocene Calc-Alkaline Volcanic Rocks from the Kastamonu Area, Northern Turkey. *Contributions to Mineralogy and Petrology*, 58 (1): 63–81. doi:10.1007/bf00384745

Richards, J. P., 2009. Postsubduction Porphyry Cu-Au and Epithermal Au Deposits: Products of Remelting of Subduction-Modified Lithosphere. *Geology*, 37(3): 247–250. doi:10.1130/g25451a.1

Rickwood, P. C., 1989. Boundary Lines within Petrologic Diagrams which Use Oxides of Major and Minor Elements. *Lithos*, 22(4): 247–263. doi:10.1016/0024-4937(89)90028-5

Shen, P., Shen, Y. C., Pan, H. D., et al., 2010. Baogutu Porphyry Cu-Mo-Au Deposit, West Junggar, Northwest China: Petrology, Alteration, and Mineralization. *Economic Geology*, 105(5): 947–970. doi:10.2113/econgeo.105.5.947

Sillitoe, R. H., 2010. Porphyry Copper Systems. *Economic Geology*, 105(1): 3–41. doi:10.2113/gsecongeo.105.1.3

Smoliar, M. I., Walker, R. J., Morgan, J. W., 1996. Re-Os Ages of Group IIA, IIIA, IVA, and IVB Iron Meteorites. *Science*, 271(5252): 1099–1102. doi:10.1126/science.271.5252.1099

Sun, S. S., McDonough, W., 1989. Chemical and Isotopic Systematics of Oceanic Basalts: Implications for Mantle Composition and Processes. *Geological Society*, *London*, *Special Publications*, 42(1): 313–345. doi:10.1144/gsl.sp.1989.042.01.19

Wakita, K., Metcalfe, I., 2005. Ocean Plate Stratigraphy in East and Southeast Asia. *Journal of Asian Earth Sciences*, 24(6): 679–702. doi:10.1016/j.jseaes.2004.04.004

Wang, F., Zhou, X. H., Zhang, L. C., et al., 2006. Late Mesozoic Volcanism in the Great Xing'an Range (NE China): Timing and Implications for the Dynamic Setting of NE Asia. *Earth and Planetary Science Letters*, 251(1): 179–198. doi:10.1016/j.epsl.2006.09.007

Wang, J. G., He, Z. H., Xu, W. L., 2013. Petrogenesis of Riebeckite Rhyolites in the Southern Da Hinggan Mts.: Geohronological and Geochemical Evidence. *Acta Petrologica Sinica*, 29(3): 853–863 (in Chinese with English Abstract)

Wang, L. T., Wang, L. B., Wang, Y. W., 2002. REE Geochemistry of the Huangguangliang Skarn Fe-Sn Deposit, Inner Mongolia. *Acta Petrologica Sinica*, 18(4): 575–584 (in Chinese with English Abstract)

Watson, E. B., Harrison, T. M., 1983. Zircon Saturation Revisited: Temperature and Composition Effects in a Variety of Crustal Magma Types. *Earth and Planetary Science Letters*, 64(2): 295–304. doi:10.1016/0012-821x(83)90211-x

Whalen, J. B., Currie, K. L., Chappell, B. W., 1987. A-Type Granites: Geochemical Characteristics, Discrimination and Petrogenesis. *Contributions to Mineralogy and Petrology*, 95(4): 407–419. doi:10.1007/bf00402202

Windley, B. F., Alexeiev, D., Xiao, W. J., et al., 2007. Tectonic Models for Accretion of the Central Asian Orogenic Belt. *Journal of the Geological Society*, 164(1): 31–47. doi:10.1144/0016-76492006-022

Wu, F. Y., Li, X. H., Yang, J. H., et al., 2007. Discussions on the Petrogenesis of Granites. *Acta Petrologica Sinica*, 23(6): 1217–1238 (in Chinese with English Abstract)

Wu, F. Y., Sun, D. Y., Zhang, G. L., et al., 2000. Deep Geodynamics of Yanshan Movement. *Geological Journal of China Universities*, 6(3): 379–388 (in Chinese with English Abstract)

Wu, G., Chen, Y. J., Sun, F. Y., et al., 2008. Geochemistry of the Late Jurassic Granitoids in the Northern End Area of Da Hinggan Mountains and Their Geological and Prospecting Implications. *Acta Petrologica Sinica*, 24(4): 899–910 (in Chinese with English Abstract)

Wu, H. Y., Zhang, L. C., Chen, Z. G., et al., 2008. Geochemistries, Tectonic Setting and Mineralization Potentiality of the Ore-Bearing Monzogranite in the Kulitu Molybdenum (Copper) Deposit of Xarmoron Metallogetic Belt, Inner Mongolra. *Acta Petrologica Sinica* 24(4): 867–878 (in Chinese with English Abstract)

Wu. F. Y., Sun, D. Y., Li, H., et al., 2002. A-Type Granites in Northeastern China: Age and Geochemical Constraints on Their Petrogenesis. *Chemical Geology*, 187(1): 143–173. doi:10.1016/s0009-2541(02)00018-9

Xin, J., 2013. The Polymetallic Metallogenic Series and Exploration Modle in the Southeast of Inner Mongolia: [Dissertation]. China University of Geosciences, Beijing. 24–26 (in Chinese with English Abstract)

Xu, F., Ren, Z. H., Zhang, B. S., 2012. Geological Characteristics of the Dongshanwan Tungsten and Molybden Mine, Balinzou Qi, Inner Mongolia. *Mineral Resource Geology*, 26(1): 24–29 (in Chinese with English Abstract)

Xu, M. J., Xu, W. L., Meng, E., et al., 2011. LA-ICP-MS Zircon U-Pb Chronology and Geochemistry of Mesozoic Volcanic Rocks from the Shanghulin-Xiangyang Basin in Ergun Area, Northeastern Inner Mongolia. *Geological Bulletin of China*, 30(9): 1321–1338 (in Chinese with English Abstract)

Xu, W. L., Ji, W. Q., Pei, F. P., et al., 2009. Triassic Volcanism in Eastern Heilongjiang and Jilin Provinces, NE China: Chronology, Geochemistry, and Tectonic Implications. *Journal of Asian Earth Sciences*, 34(3): 392–402. doi:10.1016/j.jseaes.2008.07.001

Xu, W. L., Pei, F. P., Wang, F., et al., 2013. Spatial-Temporal Relationships of Mesozoic Volcanic Rocks in NE China: Constraints on Tectonic Overprinting and Transformations between Multiple Tectonic Regimes. *Journal of Asian Earth Science*, 74: 167–193. doi:10.1016/j.jseaes.2013.04.003

Zeng, Q. D., Liu, J. M., Chu, S. X., et al., 2014. Re-Os and U-Pb Geochronology of the Duobaoshan Porphyry Cu-Mo-(Au) Deposit, Northeast China, and Its Geological Significance. *Journal of Asian Earth Sciences*, 79(2): 895–909. doi:10.1016/j.jseaes.2013.02.007

Zeng, Q. D., Liu, J. M., Qin, F., et al., 2010b. Geochronology of the Xiaodonggou Porphyry Mo Deposit in Northern Margin of North China Craton. *Resource Geology*, 60 (2): 192–202. doi:10.1111/j.1751-3928.2010.00125.x

Zeng, Q. D., Liu, J. M., Zhang, Z. L., 2010a. Re-Os Geochronology of Porphyry Molybdenum Deposit in South Segment of Da Hinggan Mountains, Northeast China. *Journal of Earth Science*, 21(4): 392–401. doi:10.1007/s12583-010-0102-4

Zeng, Q. D., Liu, J. M., Zhang, Z. L., et al., 2009. Ore-Forming Time of the Jiguanshan Porphyry Molybdenum Deposit, Northern Margin of North China Craton and the Indosinian Mineralization. *Acta Petrologica Sinica*, 25(2): 393–398 (in Chinese with English Abstract)

Zeng, Q. D., Liu, J. M., Zhang, Z. L., et al., 2011. Geology and Geochronology of the Xilamulun Molybdenum Metallogenic Belt in Eastern Inner Mongolia, China. *International Journal of Earth Sciences*, 100(8): 1791–1809. doi:10.1007/s00531-010-0617-z

Zeng, Q. D., Sun, Y., Chu, S. X., et al., 2015. Geochemistry and Geochronology of the Dongshanwan Porphyry Mo-W Deposit, Northeast China: Implications for the Late Jurassic Tectonic Setting. *Journal of Asian Earth Sciences*, 97(2): 472–485. doi:10.1016/j.jseaes.2014.07.027

Zeng, Q. D., Sun, Y., Duan, X. X., et al., 2013. U-Pb and Re-Os Geochronology of the Haolibao Porphyry Mo-Cu Deposit, NE China: Implications for a Late Permian Tectonic Setting. *Geological Magazine*, 150(6): 975–985. doi:10.1017/s0016756813000186

Zeng, Q. D., Yang, J. H., Liu, J. M., et al., 2012. Genesis of the Chehugou Mo-Bearing Granitic Complex on the Northern Margin of the North China Craton: Geochemistry, Zircon U-Pb Age and Sr-Nd-Pb Isotopes. *Geological Magazine*, 149(5): 753–767. doi:10.1017/s0016756811000987

Zhang, H. F., Parrish, R., Zhang, L., et al., 2007. A-Type Granite and Adakitic Magmatism Association in Songpan-Garze Fold Belt, Eastern Tibetan Plateau: Implication for Lithospheric Delamination. *Lithos*, 97(3): 323–335. doi:10.1016/j.lithos.2007.01.002

Zhang, J. H., 2009. Chronology and Geochemistry of the Mesozoic Volcanic Rocks in the Great Xin'an Range Northeastern China: [Dissertation]. China University of Geosciences, Wuhan. 40–56 (in Chinese with English Abstract)

Zhang, J. H., Gao, S., Ge, W. C., et al., 2010. Geochronology of the Mesozoic Volcanic Rocks in the Great Xing'an Range, Northeast China: Implications for Subduction-Induced Delamination. *Chemical Geology*, 276(3): 144–165. doi:10.1016/j.chemgeo.2010.05.013

Zhang, J. H., Ge, W. C., Wu, F. Y., et al., 2008. Large-Scale Early Cretaceous Volcanic Events in the Northern Great Xing'an Range, Northeastern China. *Lithos*, 102(1): 138–157. doi:10.1016/j.lithos.2007.08.011

Zhang, K. X., Pan, G. T., He, W. H., et al., 2016. New Division of Tectonic-Strata Superregion in China. *Earth Science—Journal of China University of Geosciences*, 40(2): 206–233 (in Chinese with English Abstract)

Zhang, L. C., Wu, H. Y., Xiang, P., et al., 2010. Ore-Forming Processes and Mineralization of Complex Tectonic System during the Mesozoic: A Case from Xilamulun Cu-Mo Metallogenic Belt. *Acta Petrologica Sinica*, 26(5): 1351–1362 (in Chinese with English Abstract)

Zhang, Q., Ran, H., Li, C. D., 2012. A-Type Granite: What is the Essence?. *Atca Petrologica Mineralogica*, 31(4): 621–626 (in Chinese with Eng-

lish Abstract)

Zhang, Y. Q., Dong, S. W., Zhao, Y., et al., 2008. Jurassic Tectonics of North China: A Synthetic View. *Acta Petrologica Sinica*, 82(2): 310–326 (in Chinese with English Abstract)

Zhang, Z. L., Zeng, Q. D., Qu, W. J., et al., 2009. The Molybdenite Re-Os Dating from the Nianzigou Mo Deposit, Inner Mongolia and its Geologial Significance. *Acta Petrologica Sinica*, 25(1): 212–218 (in Chinese with English Abstract)

Zhao, Y. M., Zhang, D. Q., 1994. Inner Mongolia Southeast of Copper Polymetallic Mineralization Geological Conditions and Prospecting Mode. Earthquake Press, Beijing. 1–722 (in Chinese)

Zhao, Y., Yang, Z. N., Ma, X. H., 1994. Geotectonic Transition from Paleoasian System and Paleotethyan System to Paleopacific Active Continental Margin in Eastern Asia. *Scientia Geologica Sinica*, 29(2): 105–119 (in Chinese with English Abstract)

Zhou, Z. H., Lü, L. S.,Yang, Y. J., et al., 2010. Petrogenesis of the Early Cretaceous A-Type Granite in the Huanggang Sn-Fe Deposit, Inner Mongolia: Constraints from Zircon U-Pb Dating and Geochemistry. *Acta Petrologica Sinica*, 26(3): 667–669 (in Chinese with English Abstract)

Zhu, Y., An, F., Feng, W., et al., 2016. Geological Evolution and Huge Ore-Forming Belts in the Core Part of the Central Asian Metallogenic Region. *Journal of Earth Science*, 27(3): 491–506